Case Studies in Thermal Engineering 28 (2021) 101453

Contents lists available at ScienceDirect

Case Studies in Thermal Engineering

journal homepage: www.elsevier.com/locate/csite

Fractional order simulations for the thermal determination of graphene oxide (GO) and molybdenum disulphide (MoS_2) nanoparticles with slip effects

Ali Raza [a], Sami Ullah Khan [b], M. Ijaz Khan [c,*], Saadia Farid [a], Taseer Muhammad [d], M. Imran Khan [e], Ahmed M. Galal [f,g]

[a] Department of Mathematics, University of Engineering and Technology, Lahore, 54890, Pakistan
[b] Department of Mathematics, COMSATS University Islamabad, Sahiwal, 57000, Pakistan
[c] Department of Mathematics and Statistics, Riphah International University I-14, Islamabad, 44000, Pakistan
[d] Department of Mathematics, College of Sciences, King Khalid University, Abha, 61413, Saudi Arabia
[e] Institute of Petroleum Engineering, Heriot Watt University, Edinburgh, UK
[f] Mechanical Engineering Department, College of Engineering, Prince Sattam Bin Abdulaziz University, Wadi addawaser, 11991, Saudi Arabia
[g] Production Engineering and Mechanical Design Department, Faculty of Engineering, Mansoura University, P.O 35516, Mansoura, Egypt

ARTICLE INFO

Keywords:
AB-fractional derivatives
Molybdenum disulphide nanoparticles
Casson fluid
Thermal radiation

ABSTRACT

In this thermal investigation, the mixed free convection Casson nanofluid along with heat transfer effects over a vertical plate is addressed. The thermal radiative phenomenon is also considered to improve the heat transfer rate. For base fluid, the engine oil is assumed for which the thermal enhancement is predicted with the suspension of graphene oxide (GO) and molybdenum disulphide (MoS_2) nanoparticles. To construct the fractional model, the partial derivative with respect to time is exchanged by the recent definitions of fractional derivatives namely Atangana-Baleanu (AB) and Caputo-Fabrizio (CF) time-fractional derivative and the Laplace scheme is applied to obtain the solution of governing equations. To enhance the innovation of this article different cases of velocity profiles are examined. The effects of different parameters are examined graphically and numerically by varying the values of parameters. The reported results claimed that the simulations performed via AB-time fractional are more stable as compared to the Caputo-Fabrizio time-fractional approach. The velocity profile declines with increasing the fractional parameters while increasing change in velocity has been observed for Grashof number. The nanoparticles temperature shows a lower change due to volume fraction coefficient.

1. Introduction

Following to the remarkable thermophysical aspects and stable features, the nanofluids offer well reputed applications in industrial and engineering sectors. The nano-materials attained ultra-high and fascinating features like viscosity, thermal conductivity and surface tension in contrast to the base materials. The inclusion of nanoparticles and base fluids improves the thermal capability of base liquids more precisely. The lack of energy resources and challenging pronounced the industrial and engineering products as many of such phenomenon involves the base fluid as an energy source. This substantial issue is solved by utilizing the nanoparticles as an

* Corresponding author.
E-mail address: ijazfmg_khan@yahoo.com (M.I. Khan).

https://doi.org/10.1016/j.csite.2021.101453
Received 25 August 2021; Received in revised form 10 September 2021; Accepted 13 September 2021
Available online 17 September 2021

Nomenclatures

w	Velocity$[m/s]$
t	Time$[s]$
U_o	Constant Velocity$[m/s]$
ρ_{nf}	Density ofnanofluid$[Kg/m^3]$
T	Non-Dimensional temperature$[K]$
k_{nf}	Thermal conductivity of nanofluid$[W/m^2k]$
Pr	Prandtl number
Gr	Grashof number
β_c	Casson parameter
μ_{nf}	Dynamic viscosity off nanofluid $[Kg/ms]$
ρ_s	Density of nanoparticles$[Kg/m^3]$
β	AB-fractional derivative operator
α	CF-fractional derivative operator
Nu	Nusselt number
C_f	Skin Friction
CF	Caputo-Fabrizio fractional derivative
β	AB-fractional parameter
q	Laplace variable by AB
s	Laplace variable by CF
g	Acceleration due to gravity$[m/s^2]$
AB	Atangana-Baleanu fractional derivative
ρ_f	Density of base fluid$[Kg/m^3]$

energy source with immersion with base fluids. Choi [1] pronounced the basic features of nanoparticles via experimental support. Siddiqui and Turkyilmazoglu [2] followed a theoretical continuation for inspecting the ferro-nanoparticles thermal prospective confined by cavity. Abbas et al. [3] worked out the hybrid nano-material flow model induced via nonlinear cylinder. Nadeem et al. [4] simulated a dual simulations fo a nanofluid problem accounted with anisotropic slip features. Khan et al. [5] explained the thermal outcomes of couple stress nanofluid subject to the slip mechanism. The viscoelastic nanofluid properties with modified porous space law with convective conditions were identified by Waqas et al. [6]. Kumar et al. [7] determined the nanofluid applications with KKL correlations over a moving curved surface with implementation of shooting technique. Khan et al. [8] visualized the modified second grade nanoparticles flow with prescribed features of nonlinear thermal radiation. Mandal and Shit [9] presented the entropy generation investigation for the biviscosity nanofluid over rotating permeable disk. The interesting numerical model for the hybrid nanoparticles over spinning disk was claimed by Acharya [10]. Zhang et al. [11] observed the thermal upshot for gold and silver nanoparticles subject to the melting applications. The 3-D nanoparticles analysis for the radiative flow of Jeffrey nanofluid was analytically worked out by Ahmad et al. [12]. Vaidya et al. [13] determined the Riga nanofluid flow with mixed convection analysis. Pourhoseini et al. [14] experimentally noticed the inclusion of Al_2O_3 nanoparticles with biodiesel base liquid results improved thermal features. Hassan et al. [15] addressed the thermal applications of hybrid nanofluid with experimental justifications. Gowda et al. [16] presented the role of slip features in the Casson-Maxwell nanofluid via stretching disks. Jamshed et al. [17] followed the single phase nanofluid model to address the thermal aspects of second grade nanofluid with radiative phenomenon. Gowda et al. [18] inspected the influence of magnetic dipole for ferromagnetic nanoparticles flow in presence of Stefan blowing constraints. Kumar et al. [19] reported the dusty fluid thermal enhancement in presence of hybrid nanoparticles confined by stretched cylinder. The computation analysis for the nanoparticles flow by following the Koo–Kleinstreuer and Li (KKL) model was identified by Gowda et al. [20].

The fractional calculus is the interesting branch of mathematics which is associated to the derivative and integrals of various types. The significant interest of researchers is developed on this topic in last some years. Different definitions of fractional derivatives with local and non-local approach are developed. The implementations of non-local derivative are more precise able due to involved function. A new types of fractional derivative is Atangana-Baleanu (AB) derivative which solved the local kernel for the Caputo-Fabrizio (CF) derivative. Many authors followed this approach to discuss the fractional simulations for various problems [21–32].

After claiming the improved thermal upshot of nanoparticles, this contribution reflects the thermal enhancement of graphene oxide (GO) and molybdenum disulphide (MoS_2) nanoparticles over vertically moving plate with help of fractional approach. The Casson liquid is assumed to be base fluid. The Casson fluid characterizes the properties of shear thinning more effectively [33–35]. Literature regarding new developments in fluid flow in view of different fluid model is listed in Refs. [36–40]. The characteristics of base fluid are referred to the engine oil applications. The fractional simulations for the formulated problem are performed with help of Atangana-Baleanu (AB) and Caputo-Fabrizio (CF) time-fractional derivative. The solution for momentum and thermal boundary layer via fractional simulations is presented. The special case for the flow motion is also considered.

2. Problem formulation

The vertical plate flow of Casson fluid has been considered Casson fluid with immersion of graphene oxide (GO) and molybdenum disulphide (MoS_2) nanoparticles. In start of simulations, ($t = 0$), the temperature is kept constant according to the atmosphere. After some time $t = 0^+$, thestationary plate starts to vibrate with constant velocity $\frac{f(t)}{\mu}$ and temperature varies to ϑ_w. Here, $f(t)$ is a non-negative function with $f(0) = 0$and having some of its Laplace transformations and also supposed that the slip exists on the boundaries of the wall and the velocity at the bottom is proportional to shear stress. With the vibration of the plate, fluid also starts to flow on the vibrating plate with the same velocity as the plate oscillates. The governing equations representing the flow of Casson fluid with nanoparticles are [26,27,33]:

$$\rho_{nf}\frac{\partial w(\xi,t)}{\partial t}=\mu_{nf}\left(1+\frac{1}{\upsilon}\right)\frac{\partial^2 w(\xi,t)}{\partial \xi^2}+g(\rho\beta)_{nf}[\vartheta(\xi,t)-\vartheta_\infty]\;;\quad \xi,t>0 \tag{1}$$

$$\left(\rho C_p\right)_{nf}\frac{\partial \vartheta(\xi,t)}{\partial t}=k_{nf}\frac{\partial^2 \vartheta(\xi,t)}{\partial \xi^2}\;;\quad \xi,t>0 \tag{2}$$

With proper its respective conditions:

$$w(\xi,0)=0,\quad \vartheta(\xi,0)=\vartheta_\infty\quad;\quad \xi>0 \tag{3}$$

$$w(\xi,t)-b\frac{\partial w(\xi,t)}{\partial \xi}=\frac{f(t)}{\mu},\quad \frac{\partial \vartheta(\xi,t)}{\partial \xi}=-\frac{h}{k}\vartheta(\xi,t)\;;\;\xi=0,\;t>0 \tag{4}$$

$$w(\xi,t)\to 0,\quad \vartheta(\xi,t)\to 0\;;\quad \xi\to\infty,\;t>0 \tag{5}$$

where

$$\mu_{nf}=\frac{\mu_f}{(1-\phi)^{2.5}},\quad \rho_{nf}=(1-\phi)\rho_f+\phi\rho_s$$

$$(\rho\beta)_{nf}=(1-\phi)(\rho\beta)_f+\phi(\rho\beta)_s\;,\quad \left(\rho C_p\right)_{nf}=(1-\phi)\left(\rho C_p\right)_f+\phi\left(\rho C_p\right)_s$$

$$\frac{k_{nf}}{k_f}=\frac{k_s+2k_f-2\phi\left(k_f-k_s\right)}{k_s+2k_f+\phi\left(k_f-k_s\right)},\quad \frac{\sigma_{nf}}{\sigma_f}=\frac{\sigma_s+2\sigma_f-2\phi\left(\sigma_f-\sigma_s\right)}{\sigma_s+2\sigma_f+\phi\left(\sigma_f-\sigma_s\right)}$$

are the dynamic viscosity, the effective density of the nanofluid, heat capacitance, thermal conductivity, electrical conductivity of the engine oil-based nanofluids. The thermal properties of engine oil, graphene oxide (GO) and molybdenum disulphide (MoS_2) nanoparticles are presented in Table 1.

Now to non-dimensionalize the respective governing equations and conditions, introducing the appropriate non-dimensional parameters as follows:

$$w^*=\frac{w}{U_o}\;,\;\xi^*=\frac{\xi U_o}{\upsilon_f}\;,\;b^*=\frac{bU_o^2}{\upsilon},\;t^*=\frac{tU_o^2}{\upsilon_f}\;,\;T^*=\frac{\vartheta-\vartheta_\infty}{\vartheta_w-\vartheta_\infty}\;,\;f^*(t^*)=\frac{1}{\mu}\sqrt{\frac{t_o}{\upsilon}}f(t_o t^*)$$

After the process of non-dimensionalization, we yield the subsequent governing equations and conditions

$$\left((1-\phi)\rho_f+\phi\frac{\rho_s}{\rho_f}\right)\frac{\partial w(\xi,t)}{\partial t}=\frac{1}{(1-\phi)^{2.5}}\left(1+\frac{1}{\upsilon}\right)\frac{\partial^2 w(\xi,t)}{\partial \xi^2}+\left((1-\phi)+\phi\frac{(\rho\beta)_s}{(\rho\beta)_f}\right)Gr\,T(\xi,t)\;;\quad \xi,t>0 \tag{6}$$

$$\left((1-\phi)+\phi\frac{\left(\rho C_p\right)_s}{\left(\rho C_p\right)_f}\right)Pr\frac{\partial T(\xi,t)}{\partial t}=\frac{k_{nf}}{k_f}\frac{\partial^2 T(\xi,t)}{\partial \xi^2}\;;\quad \xi,t>0 \tag{7}$$

with

$$w(\xi,0)=0,\quad T(\xi,0)=0\quad;\quad \xi>0 \tag{8}$$

Table 1
Physical properties of engine oil and nanoparticles [25].

Material	$\rho(Kg/m^3)$	$C_p(J/Kg\,K)$	$k(w/m.K)$	$\beta\times 10^5(1/K)$
Engine Oil	884	1910	0.144	70
GO	1800	717	5000	0.284
MoS_2	5060	397.21	904.4	2.8424

$$w(\xi,t)-b\frac{\partial w(\xi,t)}{\partial \xi}=f(t)\ ,\quad \frac{\partial T(\xi,t)}{\partial \xi}=-(1+T(\xi,t))\quad ;\quad \xi=0,\ t>0 \tag{9}$$

$$w(\xi,t)\to 0, T(\xi,t)\to 0; \xi\to\infty, t>0 \tag{10}$$

Preliminaries: To construct the fractional model recent definitions of fractional derivatives namely AB and CF-time fractional derivative are utilized, whose mathematical form is defined as [26] for the function $f(\xi,t)$

$${}^{AB}\mathfrak{D}_t^{\beta}f(\xi,t)=\frac{1}{1-\beta}\int_0^t E_{\beta}\left[\frac{\beta(t-z)^{\beta}}{1-\beta}\right]f'_{(\xi,t)}dt \tag{11}$$

with its Laplace transformation [27].

$$\mathscr{L}\left\{{}^{AB}\mathfrak{D}_t^{\beta}f(\xi,t)\right\}=\frac{q^{\beta}\mathscr{L}[f(\xi,t)]-q^{\beta-1}f(\xi,0)}{(1-\beta)q^{\beta}+\beta} \tag{12}$$

The mathematical definition of CF-time fractional derivative for the function $f(\xi,t)$ is

$${}^{CF}\mathfrak{D}_t^{\alpha}f(\xi,t)=\frac{1}{1-\alpha}\int_0^t exp\left(\frac{\alpha(1-\tau)}{1-\alpha}\right)f'(\xi,t)d\tau \tag{13}$$

With its Laplace as [28,29]:

$$\mathscr{L}\left\{{}^{CF}\mathfrak{D}_t^{\alpha}f(\xi,t)\right\}=\frac{s\mathscr{L}[f(\xi,t)]-f(\xi,0)}{(1-\alpha)s+\alpha} \tag{14}$$

3. Modeling with AB-time fractional derivative

The fraction modal with the definition of AB-fractional derivative (11) can be formulated by replacing the partial derivative w.r.t time of transformed equations (6) and (7) by ${}^{AB}\mathfrak{D}_t^{\beta}$ which is the operator of AB-fractional derivative

$$\Lambda_1\,{}^{AB}\mathfrak{D}_t^{\beta}w(\xi,t)=\Lambda_2\beta_c\frac{\partial^2 w(\xi,t)}{\partial\xi^2}+\Lambda_3 GrT(\xi,t), \tag{15}$$

$$\Lambda_4 Pr\,{}^{AB}\mathfrak{D}_t^{\beta}T(\xi,t)=\Lambda_5\frac{\partial^2 T(\xi,t)}{\partial\xi^2}, \tag{16}$$

where

$$\Lambda_1=(1-\phi)\rho_f+\phi\frac{\rho_s}{\rho_f}\ ,\quad \Lambda_2=\frac{1}{(1-\phi)^{2.5}}\ ,\quad \Lambda_3=(1-\phi)+\phi\frac{(\rho\beta)_s}{(\rho\beta)_f}$$

$$\Lambda_4=(1-\phi)+\phi\frac{(\rho C_p)_s}{(\rho C_p)_f}\ ,\quad \Lambda_5=\frac{k_{nf}}{k_f}\ ,\quad \beta_c=1+\frac{1}{\upsilon}$$

3.1. Energy equation via AB-fractional derivative

By applying the Laplace definition on AB-fractional model equation (16) for the solution of energy equation and on its corresponding conditions

$$\Lambda_4 Pr\left(\frac{q^{\beta}\mathscr{L}[T(\xi,t)]-q^{\beta-1}T(\xi,0)}{(1-\beta)q^{\beta}+\beta}\right)=\Lambda_5\frac{\partial^2\overline{T}(\xi,q)}{\partial\xi^2}, \tag{17}$$

Where $\overline{T}(\xi,q)$ is the Laplace of $T(\xi,t)$, with respective conditions

$$\left.\frac{\partial\overline{T}}{\partial\xi}\right|_{\xi=0}=-\left(\frac{1}{q}+\overline{T}(0,q)\right)\ ,\quad \overline{T}(\xi,q)\to 0\ as\ \xi\to\infty.$$

By introducing the above conditions, the solution of the energy equation will be

$$\overline{T}(\xi,q)=\frac{1}{\left(\sqrt{\frac{\Lambda_4 Pr}{\Lambda_5}\frac{q^{\beta}}{(1-\beta)q^{\beta}+\beta}}-1\right)}\frac{e^{-\xi\sqrt{\frac{\Lambda_4 Pr}{\Lambda_5}\frac{q^{\beta}}{(1-\beta)q^{\beta}+\beta}}}}{q} \tag{18}$$

The Laplace inverse of equation (18) will be analyzed numerically by Stehfest and Zakians methods in Table 2.

3.1.1. Momentum equation via AB-fractional derivative

For the solution of the momentum equation, applying the Laplace transformation on equation (15) and its respective transformed boundary conditions.

$$\Lambda_1\left(\frac{q^{\beta}\mathscr{L}[w(\xi,t)]-q^{\beta-1}w(\xi,0)}{(1-\beta)q^{\beta}+\beta}\right)=\Lambda_2\beta_c\frac{\partial^2\overline{w}(\xi,q)}{\partial\xi^2}+\Lambda_3 Gr\overline{T}(\xi,q), \tag{19}$$

with:

$$\overline{w}(\xi,q)-b\frac{\partial\overline{w}(\xi,q)}{\partial\xi}=F(q)\ as\ \xi=0,$$

$$\overline{w}(\xi,q)\to 0 as\ \xi\to\infty. \tag{20}$$

Simplifying equation (19) and using the above conditions we yield the solution of the momentum equation as follows

$$\begin{aligned}\overline{w}(\xi,q)=&\frac{1}{1+b\sqrt{\frac{\Lambda_1}{\Lambda_2\beta_c}\frac{q^{\beta}}{(1-\beta)q^{\beta}+\beta}}}\left(\frac{\Lambda_3 Gr}{\Lambda_2\beta_c}\frac{1}{q\left(\sqrt{\frac{\Lambda_4 Pr}{\Lambda_5}\frac{q^{\beta}}{(1-\beta)q^{\beta}+\beta}}-1\right)}\frac{1+b\sqrt{\frac{\Lambda_4 Pr}{\Lambda_5}\frac{q^{\beta}}{(1-\beta)q^{\beta}+\beta}}}{\left(\frac{\Lambda_4 Pr}{\Lambda_5}-\frac{\Lambda_1}{\Lambda_2\beta_c}\right)\left(\frac{q^{1+\beta}}{(1-\beta)q^{\beta}+\beta}\right)}+F(q)\right)e^{-\xi\sqrt{\frac{\Lambda_1}{\Lambda_2\beta_c}\frac{q^{\beta}}{(1-\beta)q^{\beta}+\beta}}}\\&-\frac{\Lambda_3 Gr}{\Lambda_2\beta_c}\frac{1}{q\left(\sqrt{\frac{\Lambda_4 Pr}{\Lambda_5}\frac{q^{\beta}}{(1-\beta)q^{\beta}+\beta}}-1\right)}\frac{e^{-\xi\sqrt{\frac{\Lambda_4 Pr}{\Lambda_5}\frac{q^{\beta}}{(1-\beta)q^{\beta}+\beta}}}}{\left(\frac{\Lambda_4 Pr}{\Lambda_5}-\frac{\Lambda_1}{\Lambda_2\beta_c}\right)\left(\frac{q^{1+\beta}}{(1-\beta)q^{\beta}+\beta}\right)}\end{aligned} \tag{21}$$

4. Modeling with CF-time fractional derivative

For the fractional model of CF-time fractional derivative replacing the partial derivative w.r.t time by CF-fractional operator ${}^{CF}\mathfrak{D}_t^{\alpha}$, we obtain the following governing equations

$$\Lambda_1\,{}^{CF}\mathfrak{D}_t^{\alpha}w(\xi,t)=\Lambda_2\beta_c\frac{\partial^2 w(\xi,t)}{\partial\xi^2}+\Lambda_3 GrT(\xi,t) \tag{22}$$

$$\Lambda_4 Pr\,{}^{CF}\mathfrak{D}_t^{\alpha}T(\xi,t)=\Lambda_5\frac{\partial^2 T(\xi,t)}{\partial\xi^2};\ \xi,t>0 \tag{23}$$

With transformed conditions

$$w(\xi,0)=0,\quad T(\xi,0)=0\quad;\quad \xi>0$$

$$w(\xi,t)-b\frac{\partial w(\xi,t)}{\partial\xi}=f(t),\quad \left.\frac{\partial T}{\partial\xi}\right|_{\xi=0}=-(1+T(0,t))\,;\quad \xi=0,\ t>0$$

Table 2
Analysis of temperature and Nusselt number with the variation in fractional parameter.

α,β	Temp (*AB*)	Temp (*CF*)	*Nu* (*AB*)	*Nu* (*CF*)
0.1	0.6076	0.6055	2.4256	2.5573
0.2	0.5986	0.5905	2.4821	2.6739
0.3	0.5784	0.5620	2.5691	2.7777
0.4	0.5455	0.5199	2.6776	2.8701
0.5	0.5006	0.4664	2.7961	2.9521
0.6	0.4459	0.4047	2.9129	3.0249
0.7	0.3843	0.3381	3.0177	3.0890
0.8	0.3180	0.2688	3.1033	3.1447
0.9	0.2486	0.1982	3.1656	3.1924

$$w(\xi,t)\to 0,\quad T(\xi,t)\to 0\quad ;\quad \xi\to\infty,\ t>0$$

4.1. Energy equation via CF-fractional derivative

As the energy equation (23) is independent of momentum profile so by applying the Laplace on equation (23)

$$\Lambda_4 Pr\left(\frac{s\mathscr{L}[T(\xi,t)]-T(\xi,0)}{(1-\alpha)s+\alpha}\right)=\Lambda_5\frac{\partial^2\overline{T}(\xi,t)}{\partial\xi^2} \tag{24}$$

where $\overline{T}(\xi,s)$ is the Laplace of $T(\xi,t)$, with the following transformed conditions:

$$\left.\frac{\partial\overline{T}}{\partial\xi}\right|_{\xi=0}=-\left(\frac{1}{s}+\overline{T}(0,s)\right),\quad \overline{T}(\xi,s)\to 0\ as\ \xi\to\infty$$

By utilizing these conditions, we attained the solution of temperature distribution as

$$\overline{T}(\xi,s)=\frac{1}{s\left(\sqrt{\frac{\Lambda_4 Pr}{\Lambda_5}\frac{s}{(1-\alpha)s+\alpha}}-1\right)}e^{-\xi\sqrt{\frac{\Lambda_4 Pr}{\Lambda_5}\frac{s}{(1-\alpha)s+\alpha}}} \tag{25}$$

The inverse of Laplace of Eq. (25) will be shortened numerically in Table 2.

4.2. Momentum equation via CF-fractional derivative

Eq. (22) is a partial differential equation of CF-time fractional modal, so utilizing the Laplace transformation on equation (22), we get

$$\Lambda_1\left(\frac{s\mathscr{L}[w(\xi,t)]-w(\xi,0)}{(1-\alpha)s+\alpha}\right)=\Lambda_2\beta_c\frac{\partial^2\overline{w}(\xi,s)}{\partial\xi^2}+\Lambda_3 Gr\overline{T}(\xi,s) \tag{26}$$

With the following transformed conditions

$$\overline{w}(\xi,s)-b\frac{\partial\overline{w}(\xi,s)}{\partial\xi}=F(s)\ as\ \xi=0$$

$$\overline{w}(\xi,s)\to 0 as\xi\to\infty \tag{27}$$

The following solution of Eq. (26) can be accomplished by exploiting the above condition (27)

$$\begin{aligned}\overline{w}(\xi,s)=&\frac{1}{1+b\sqrt{\frac{\Lambda_1}{\Lambda_2\beta_c}\frac{s}{(1-\alpha)s+\alpha}}}\left(\frac{\Lambda_3\ Gr}{\Lambda_2\beta_c}\frac{1}{s\left(\sqrt{\frac{\Lambda_4\ Pr}{\Lambda_5}\frac{s}{(1-\alpha)s+\alpha}}-1\right)}\frac{1+b\sqrt{\frac{\Lambda_4\ Pr}{\Lambda_5}\frac{s}{(1-\alpha)s+\alpha}}}{\left(\frac{\Lambda_4\ Pr}{\Lambda_5}-\frac{\Lambda_1}{\Lambda_2\beta_c}\right)\left(\frac{s}{(1-\alpha)s+\alpha}\right)}+F(s)\right)e^{-\xi\sqrt{\frac{\Lambda_1}{\Lambda_2\beta_c}\frac{s}{(1-\alpha)s+\alpha}}}\\&-\frac{\Lambda_3\ Gr}{\Lambda_2\beta_c}\frac{1}{s\left(\sqrt{\frac{\Lambda_4\ Pr}{\Lambda_5}\frac{s}{(1-\alpha)s+\alpha}}-1\right)}\frac{e^{-\xi\sqrt{\frac{\Lambda_4\ Pr}{\Lambda_5}\frac{s}{(1-\alpha)s+\alpha}}}}{\left(\frac{\Lambda_4\ Pr}{\Lambda_5}-\frac{\Lambda_1}{\Lambda_2\beta_c}\right)\left(\frac{s}{(1-\alpha)s+\alpha}\right)}\end{aligned} \tag{28}$$

For the inverse of Laplace of the velocity field via AB and CF-fractional derivative of Eqs. (21) and (28) respectively, we will use the numerical methods i.e. Grave Stehfest and Zakians method [30–32]:

$$w(\xi,t)=\frac{ln(2)}{t}\sum_{n=1}^{M}v_n\overline{w}\left(\xi,n\frac{ln(2)}{t}\right)$$

where M will be a positive integer. Moreover:

$$v_n = (-1)^{n+\frac{M}{2}} \sum_{p=\frac{q+1}{2}}^{min\left(q,\frac{M}{2}\right)} \frac{p^{\frac{M}{2}}(2p)!}{\left(\frac{M}{2}-p\right)!p!\,(p-1)!\,(q-p)!\,(2p-q)!}$$

and

$$w(\xi,t) = \frac{2}{t}\sum_{j=1}^{N} Re\left(k_j \,.\, \overline{w}\left(\xi, \frac{\alpha_j}{t}\right)\right)$$

are the Stehfest and Zakians methods respectively.

4.2.1. Special cases

As the solution of momentum field via AB and CF-fractional derivative in Eqs. (21) and (28) respectively, are in a more general form. Therefore, to illustrate some more physical insight into the problem, here we will discuss some special cases for the function $f(t)$. So here we will discuss some special cases for the velocity profile in the ramped wall case whose physical interpretation is well known in the literature.

Case 1. $f(t) = t$

In the first case, take $f(t) = t$ then the expressions of velocity field by AB and CF-fractional derivative with Eqs. (21) and (28) respectively will become as

$$\overline{w}(\xi,q) = \frac{1}{1+b\sqrt{\frac{\Lambda_1}{\Lambda_2\beta_c}\frac{q^\beta}{(1-\beta)q^\beta+\beta}}}\left(\frac{\Lambda_3\,Gr}{\Lambda_2\beta_c}\frac{1}{\left(\sqrt{\frac{\Lambda_4\,Pr}{\Lambda_5}\frac{q^\beta}{(1-\beta)q^\beta+\beta}}-1\right)}\frac{1+b\sqrt{\frac{\Lambda_4\,Pr}{\Lambda_5}\frac{q^\beta}{(1-\beta)q^\beta+\beta}}}{\left(\frac{\Lambda_4\,Pr}{\Lambda_5}-\frac{\Lambda_1}{\Lambda_2\beta_c}\right)\left(\frac{q^{1+\beta}}{(1-\beta)q^\beta+\beta}\right)}+\frac{1}{q^2}\right)e^{-\xi\sqrt{\frac{\Lambda_1}{\Lambda_2\beta_c}\frac{q^\beta}{(1-\beta)q^\beta+\beta}}}$$
$$-\frac{\Lambda_3\,Gr}{\Lambda_2\beta_c}\frac{1}{\left(\sqrt{\frac{\Lambda_4\,Pr}{\Lambda_5}\frac{q^\beta}{(1-\beta)q^\beta+\beta}}-1\right)}\frac{e^{-\xi\sqrt{\frac{\Lambda_4\,Pr}{\Lambda_5}\frac{q^\beta}{(1-\beta)q^\beta+\beta}}}}{\left(\frac{\Lambda_4\,Pr}{\Lambda_5}-\frac{\Lambda_1}{\Lambda_2\beta_c}\right)\left(\frac{q^{1+\beta}}{(1-\beta)q^\beta+\beta}\right)} \tag{29}$$

and

$$\overline{w}(\xi,s) = \frac{1}{1+b\sqrt{\frac{\Lambda_1}{\Lambda_2\beta_c}\frac{s}{(1-\alpha)s+\alpha}}}\left(\frac{\Lambda_3\,Gr}{\Lambda_2\beta_c}\frac{1}{s\left(\sqrt{\frac{\Lambda_4\,Pr}{\Lambda_5}\frac{s}{(1-\alpha)s+\alpha}}-1\right)}\frac{1+b\sqrt{\frac{\Lambda_4\,Pr}{\Lambda_5}\frac{s}{(1-\alpha)s+\alpha}}}{\left(\frac{\Lambda_4\,Pr}{\Lambda_5}-\frac{\Lambda_1}{\Lambda_2\beta_c}\right)\left(\frac{s}{(1-\alpha)s+\alpha}\right)}+\frac{1}{s^2}\right)e^{-\xi\sqrt{\frac{\Lambda_1}{\Lambda_2\beta_c}\frac{s}{(1-\alpha)s+\alpha}}}$$
$$-\frac{\Lambda_3\,Gr}{\Lambda_2\beta_c}\frac{1}{s\left(\sqrt{\frac{\Lambda_4\,Pr}{\Lambda_5}\frac{s}{(1-\alpha)s+\alpha}}-1\right)}\frac{e^{-\xi\sqrt{\frac{\Lambda_4\,Pr}{\Lambda_5}\frac{s}{(1-\alpha)s+\alpha}}}}{\left(\frac{\Lambda_4\,Pr}{\Lambda_5}-\frac{\Lambda_1}{\Lambda_2\beta_c}\right)\left(\frac{s}{(1-\alpha)s+\alpha}\right)} \tag{30}$$

Case 2. $f(t) = Sin(\omega t)$

In the second case, take $(t) = Sin(\,t)$ where ω represents the strength of the shear stress, then the expressions of velocity field by AB and CF-fractional derivative with Eqs. (21) and (28) become:

$$\overline{w}(\xi,q) = \frac{1}{1+b\sqrt{\frac{\Lambda_1}{\Lambda_2\beta_c}\frac{q^\beta}{(1-\beta)q^\beta+\beta}}}\left(\frac{\Lambda_3\,Gr}{\Lambda_2\beta_c}\frac{1}{\left(\sqrt{\frac{\Lambda_4\,Pr}{\Lambda_5}\frac{q^\beta}{(1-\beta)q^\beta+\beta}}-1\right)}\frac{1+b\sqrt{\frac{\Lambda_4\,Pr}{\Lambda_5}\frac{q^\beta}{(1-\beta)q^\beta+\beta}}}{\left(\frac{\Lambda_4\,Pr}{\Lambda_5}-\frac{\Lambda_1}{\Lambda_2\beta_c}\right)\left(\frac{q^{1+\beta}}{(1-\beta)q^\beta+\beta}\right)}+\frac{\omega}{\omega^2+q^2}\right)e^{-\xi\sqrt{\frac{\Lambda_1}{\Lambda_2\beta_c}\frac{q^\beta}{(1-\beta)q^\beta+\beta}}}$$
$$-\frac{\Lambda_3\,Gr}{\Lambda_2\beta_c}\frac{1}{\left(\sqrt{\frac{\Lambda_4\,Pr}{\Lambda_5}\frac{q^\beta}{(1-\beta)q^\beta+\beta}}-1\right)}\frac{e^{-\xi\sqrt{\frac{\Lambda_4\,Pr}{\Lambda_5}\frac{q^\beta}{(1-\beta)q^\beta+\beta}}}}{\left(\frac{\Lambda_4\,Pr}{\Lambda_5}-\frac{\Lambda_1}{\Lambda_2\beta_c}\right)\left(\frac{q^{1+\beta}}{(1-\beta)q^\beta+\beta}\right)} \tag{31}$$

and

$$\overline{w}(\xi,s)=\frac{1}{1+b\sqrt{\frac{\Lambda_1}{\Lambda_2\beta_c}\frac{s}{(1-\alpha)s+\alpha}}}\left(\frac{\Lambda_3\,Gr}{\Lambda_2\beta_c}\frac{1}{s\left(\sqrt{\frac{\Lambda_4\,Pr}{\Lambda_5}\frac{s}{(1-\alpha)s+\alpha}}-1\right)}\frac{1+b\sqrt{\frac{\Lambda_4\,Pr}{\Lambda_5}\frac{s}{(1-\alpha)s+\alpha}}}{\left(\frac{\Lambda_4\,Pr}{\Lambda_5}-\frac{\Lambda_1}{\Lambda_2\beta_c}\right)\left(\frac{s}{(1-\alpha)s+\alpha}\right)}+\frac{\omega}{\omega^2+s^2}\right)e^{-\xi\sqrt{\frac{\Lambda_1}{\Lambda_2\beta_c}\frac{s}{(1-\alpha)s+\alpha}}}$$
$$-\frac{\Lambda_3\,Gr}{\Lambda_2\beta_c}\frac{1}{s\left(\sqrt{\frac{\Lambda_4\,Pr}{\Lambda_5}\frac{s}{(1-\alpha)s+\alpha}}-1\right)}\frac{e^{-\xi\sqrt{\frac{\Lambda_4\,Pr}{\Lambda_5}\frac{s}{(1-\alpha)s+\alpha}}}}{\left(\frac{\Lambda_4\,Pr}{\Lambda_5}-\frac{\Lambda_1}{\Lambda_2\beta_c}\right)\left(\frac{s}{(1-\alpha)s+\alpha}\right)} \quad (32)$$

Case 3. $f(t)=t\,Cos(t)$

In the fourth case, take $f(t)=t\,Cos(\,t)$ with its Laplace $F(q)=\frac{q^2-1}{(q^2+1)^2}$ then the expressions of velocity field by AB and CF-fractional derivative with Eqs. (21) and (28) respectively will become as

$$\overline{w}(\xi,q)=\frac{1}{1+b\sqrt{\frac{\Lambda_1}{\Lambda_2\beta_c}\frac{q^\beta}{(1-\beta)q^\beta+\beta}}}\left(\frac{\Lambda_3\,Gr}{\Lambda_2\beta_c}\frac{1}{\left(\sqrt{\frac{\Lambda_4\,Pr}{\Lambda_5}\frac{q^\beta}{(1-\beta)q^\beta+\beta}}-1\right)}\frac{1+b\sqrt{\frac{\Lambda_4\,Pr}{\Lambda_5}\frac{q^\beta}{(1-\beta)q^\beta+\beta}}}{\left(\frac{\Lambda_4\,Pr}{\Lambda_5}-\frac{\Lambda_1}{\Lambda_2\beta_c}\right)\left(\frac{q^{1+\beta}}{(1-\beta)q^\beta+\beta}\right)}+\frac{q^2-1}{(1+q^2)^2}\right)e^{-\xi\sqrt{\frac{\Lambda_1}{\Lambda_2\beta_c}\frac{q^\beta}{(1-\beta)q^\beta+\beta}}}$$
$$-\frac{\Lambda_3\,Gr}{\Lambda_2\beta_c}\frac{1}{\left(\sqrt{\frac{\Lambda_4\,Pr}{\Lambda_5}\frac{q^\beta}{(1-\beta)q^\beta+\beta}}-1\right)}\frac{e^{-\xi\sqrt{\frac{\Lambda_4\,Pr}{\Lambda_5}\frac{q^\beta}{(1-\beta)q^\beta+\beta}}}}{\left(\frac{\Lambda_4\,Pr}{\Lambda_5}-\frac{\Lambda_1}{\Lambda_2\beta_c}\right)\left(\frac{q^{1+\beta}}{(1-\beta)q^\beta+\beta}\right)} \quad (33)$$

and

$$\overline{w}(\xi,s)=\frac{1}{1+b\sqrt{\frac{\Lambda_1}{\Lambda_2\beta_c}\frac{s}{(1-\alpha)s+\alpha}}}\left(\frac{\Lambda_3\,Gr}{\Lambda_2\beta_c}\frac{1}{s\left(\sqrt{\frac{\Lambda_4\,Pr}{\Lambda_5}\frac{s}{(1-\alpha)s+\alpha}}-1\right)}\frac{1+b\sqrt{\frac{\Lambda_4\,Pr}{\Lambda_5}\frac{s}{(1-\alpha)s+\alpha}}}{\left(\frac{\Lambda_4\,Pr}{\Lambda_5}-\frac{\Lambda_1}{\Lambda_2\beta_c}\right)\left(\frac{s}{(1-\alpha)s+\alpha}\right)}+\frac{s^2-1}{(1+s^2)^2}\right)e^{-\xi\sqrt{\frac{\Lambda_1}{\Lambda_2\beta_c}\frac{s}{(1-\alpha)s+\alpha}}}$$
$$-\frac{\Lambda_3\,Gr}{\Lambda_2\beta_c}\frac{1}{s\left(\sqrt{\frac{\Lambda_4\,Pr}{\Lambda_5}\frac{s}{(1-\alpha)s+\alpha}}-1\right)}\frac{e^{-\xi\sqrt{\frac{\Lambda_4\,Pr}{\Lambda_5}\frac{s}{(1-\alpha)s+\alpha}}}}{\left(\frac{\Lambda_4\,Pr}{\Lambda_5}-\frac{\Lambda_1}{\Lambda_2\beta_c}\right)\left(\frac{s}{(1-\alpha)s+\alpha}\right)} \quad (34)$$

Case 4. $f(t)=t\,e^t$

In the final case, take $f(t)=te^t$ with its Laplace $F(q)=\frac{1}{(q-1)^2}$then the expressions of velocity field by AB and CF-fractional derivative with Eqs. (21) and (28) respectively will become as

$$\overline{w}(\xi,q)=\frac{1}{1+b\sqrt{\frac{\Lambda_1}{\Lambda_2\beta_c}\frac{q^\beta}{(1-\beta)q^\beta+\beta}}}\left(\frac{\Lambda_3\,Gr}{\Lambda_2\beta_c}\frac{1}{\left(\sqrt{\frac{\Lambda_4\,Pr}{\Lambda_5}\frac{q^\beta}{(1-\beta)q^\beta+\beta}}-1\right)}\frac{1+b\sqrt{\frac{\Lambda_4\,Pr}{\Lambda_5}\frac{q^\beta}{(1-\beta)q^\beta+\beta}}}{\left(\frac{\Lambda_4\,Pr}{\Lambda_5}-\frac{\Lambda_1}{\Lambda_2\beta_c}\right)\left(\frac{q^{1+\beta}}{(1-\beta)q^\beta+\beta}\right)}+\frac{1}{(q-1)^2}\right)e^{-\xi\sqrt{\frac{\Lambda_1}{\Lambda_2\beta_c}\frac{q^\beta}{(1-\beta)q^\beta+\beta}}}$$
$$-\frac{\Lambda_3\,Gr}{\Lambda_2\beta_c}\frac{1}{\left(\sqrt{\frac{\Lambda_4\,Pr}{\Lambda_5}\frac{q^\beta}{(1-\beta)q^\beta+\beta}}-1\right)}\frac{e^{-\xi\sqrt{\frac{\Lambda_4\,Pr}{\Lambda_5}\frac{q^\beta}{(1-\beta)q^\beta+\beta}}}}{\left(\frac{\Lambda_4\,Pr}{\Lambda_5}-\frac{\Lambda_1}{\Lambda_2\beta_c}\right)\left(\frac{q^{1+\beta}}{(1-\beta)q^\beta+\beta}\right)} \quad (35)$$

and

$$\overline{w}(\xi,s)=\frac{1}{1+b\sqrt{\frac{\Lambda_1}{\Lambda_2\beta_c}\frac{s}{(1-\alpha)s+\alpha}}}\left(\frac{\Lambda_3\,Gr}{\Lambda_2\beta_c}\frac{1}{s\left(\sqrt{\frac{\Lambda_4\,Pr}{\Lambda_5}\frac{s}{(1-\alpha)s+\alpha}}-1\right)}\frac{1+b\sqrt{\frac{\Lambda_4\,Pr}{\Lambda_5}\frac{s}{(1-\alpha)s+\alpha}}}{\left(\frac{\Lambda_4\,Pr}{\Lambda_5}-\frac{\Lambda_1}{\Lambda_2\beta_c}\right)\left(\frac{s}{(1-\alpha)s+\alpha}\right)}+\frac{1}{(s-1)^2}\right)e^{-\xi\sqrt{\frac{\Lambda_1}{\Lambda_2\beta_c}\frac{s}{(1-\alpha)s+\alpha}}}$$
$$-\frac{\Lambda_3\,Gr}{\Lambda_2\beta_c}\frac{1}{s\left(\sqrt{\frac{\Lambda_4\,Pr}{\Lambda_5}\frac{s}{(1-\alpha)s+\alpha}}-1\right)}\frac{e^{-\xi\sqrt{\frac{\Lambda_4\,Pr}{\Lambda_5}\frac{s}{(1-\alpha)s+\alpha}}}}{\left(\frac{\Lambda_4\,Pr}{\Lambda_5}-\frac{\Lambda_1}{\Lambda_2\beta_c}\right)\left(\frac{s}{(1-\alpha)s+\alpha}\right)} \tag{36}$$

5. Results and discussion

The main objective of this analysis is to inspect the thermal significances of graphene oxide (GO) and molybdenum disulphide (MoS_2) nanoparticles by using the Atangana-Baleanu and Caputo-Fabrizio time-fractional derivatives. The solution of partial differential governing equations is obtained by applying the Laplace scheme. The effects of different constraints on leading equations are examined graphically by using math software Mathematica and the numerical analysis of Nusselt number and skin friction is also examined. For the inverse of Laplace transformation different numerical inverse techniques, i.e. Grave Stehfest algorithm and Zakians methods are exploited. The whole analysis is performed by assigning some constants values of parameters like $\phi = 0.04,\ Pr = 1.5,\ Gr = 0.75,\ \phi = 0.04,\ h = 0.5,\ t = 0.3.\alpha = 0.4,\ \beta = 0.4$. Fig. 1 is sketched for the schematic analysis of flow over a surface. The effects of fractional constraint $\alpha,\beta$and Prandtl number Pron the temperature distribution via AB and CF fractional derivatives are examined in Fig. 2 (a) and (b) for altered values of the fractional constraint and Prandtl number Pr. The behavior of temperature profile for changed values α,β presents that temperature decays by varying the values of fractional parameters and the temperature field also decrease by varying the values of the Prandtl number. Physically, enhancement in the values of Prdecreases the thermal conductivity and increases the viciousness of the fluid due to which the temperature of the nanofluid decreases by enhancing the value of Pr. In Fig. 3(a) and (b) the possessions of volume fraction ϕon temperature distribution and the comparison of ordinary temperature and fractional derivative (AB and CF) temperature are displayed for $\alpha,\beta \to 1$ respectively. Physically, enhancement in volume fraction values escalates the thermal conductivity which causes the addition of temperature field. While in comparison with ordinary and fractional model temperature, it overlaps on ordinary derivative when $\alpha,\beta \to 1$in Fig. 3(b). The overlapping of curves represents the validity of our obtained results by different numerical inverse methods.

The velocity profile via AB and CF fractional derivatives for the fractional constraints$\alpha,\beta,$ and Prandtl number $Pr$are analyzed in Fig. 4(a) and (b). It can be seen that the velocity profile decays by variation in both parameters values fractional parameter and Prandtl number. Furthermore, the velocity profile by CF-fractional derivative decays more rapidly as compared to AB-fractional derivative and altered with the increase in time. The behavior of Grashof number $Gr$and volume fraction$\phi$is examined for the velocity field of both fractional techniques. Variation in Grashof number causes enhancement in buoyancy effect which speed up the fluid velocity and surface slip decreases the fluid velocity as shown in Fig. 5(a–b). While variation in volume fraction varies the viscous effect of the fluid causes to addition in friction to flow and fluid slow down. The comparison of slip parameter and the comparison of the velocity field for

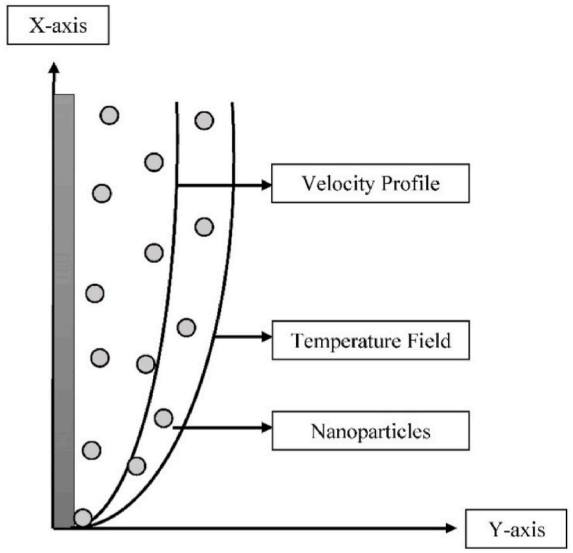

Fig. 1. Geometry of flow.

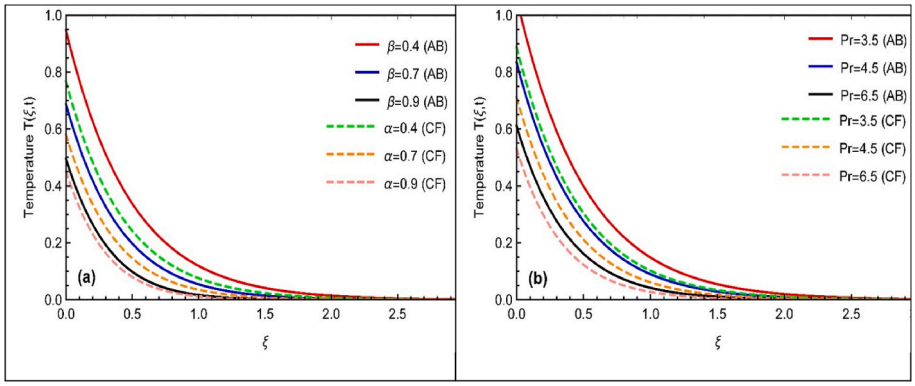

Fig. 2. (a–b):Temperature field with the variation in **(a):**fractional constraintα, β and**(b):**Prandtl number with $\phi = 0.04$, $Pr = 1.5$, $t = 0.3$.

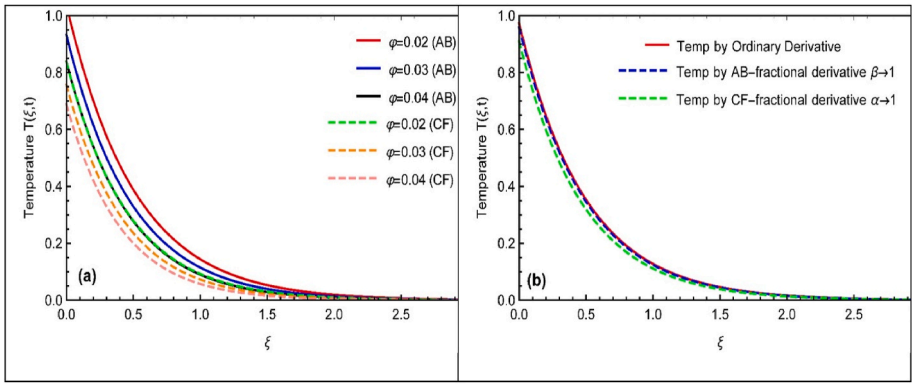

Fig. 3. (a–b):Temperature field with the variation in **(a)**volume fraction and **(b):**comparison with ordinary temperature.

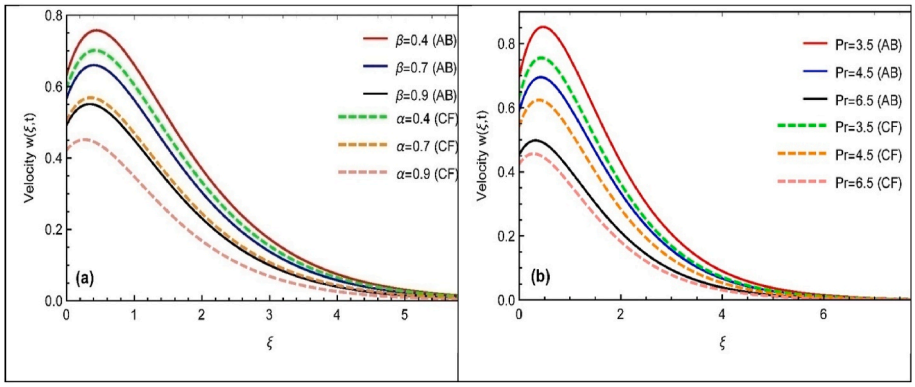

Fig. 4. (a–b):Velocity field with variation in **(a):** fractional constraint α, β and**(b):**Prandtl number with $h = 0.5$, $Gr = 0.75$, $\phi = 0.04$, $t = 0.3$.

different nanoparticles is analyzed in Fig. 6(a) and (b) respectively. The velocity of CF-time fractional derivative relatively more decays as compared to AB-time fractional derivative model velocity. Furthermore, the velocity of (MoS_2)based nanoparticles more decay as compared to (GO)based nanoparticles. Finally, the comparison of numerical techniques namely the Stehfest and Zakians method and the comparison of fractional model velocity with ordinary derivative model velocity is plotted in Fig. 7(a) and (b) respectively. It is seen that the curves of both numerical techniques overlap each other which proves the validity of obtained results. When the values of fractional parameter tend to be 1 then the curves of both fractional models overlap to ordinary velocity model which also signifies the validation of velocity profile results. Table 2 presents the variations in Nusselt number against α and. A lower change is heat transfer rate is noted for both parameters. Table 3 predicts the variation of skin friction coefficient for α, β at different time instants. The numerical simulations are performed for both Atangana-Baleanu (AB) and Caputo-Fabrizio (CF) derivatives. With increasing α and β,

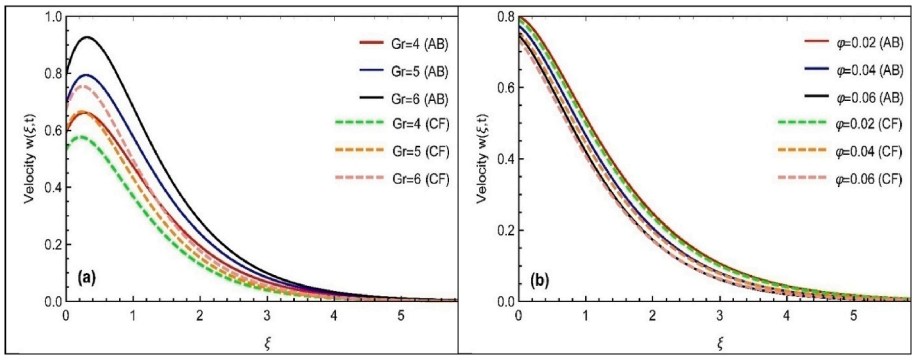

Fig. 5. (a–b): Velocity field with variation in **(a):**Grashof number and **(b):**volume fraction with $\alpha, \beta = 0.5$, $h = 0.5$, $Pr = 1.5$, $t = 0.3$.

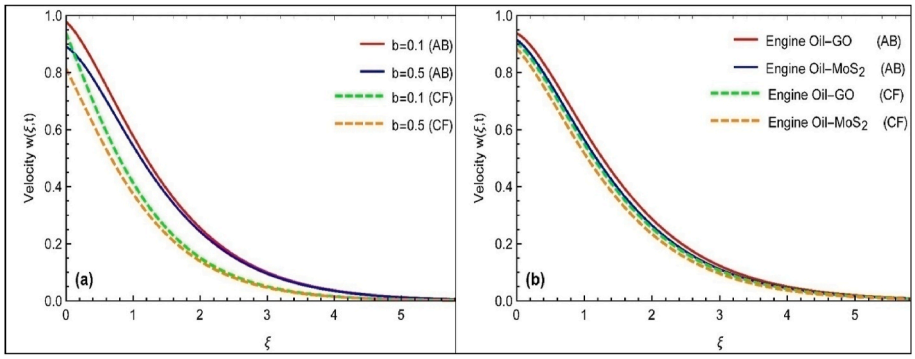

Fig. 6. (a–b): Velocity field with variation in **(a):** slip parameter and **(b):** comparison of nanoparticles.

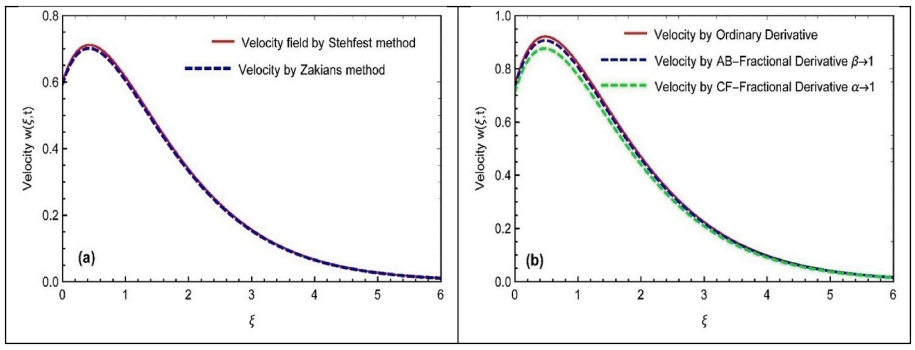

Fig. 7. (a–b): Velocity field with**(a):**comparison of numerical methods and **(b):**comparison with the ordinary velocity.

Table 3
Analysis of skin friction C_f with variation in the fractional parameter at different times by AB and CF fractional derivative.

α, β	C_f (AB) $t = 1.2$	C_f (CF) $t = 1.2$	C_f (AB) $t = 1.5$	C_f (CF) $t = 1.5$	C_f (AB) $t = 1.7$	C_f (CF) $t = 1.7$
0.1	0.5836	0.6146	0.6518	0.6284	0.6430	0.5962
0.2	0.5709	0.6100	0.6275	0.6000	0.6110	0.5414
0.3	0.5560	0.6082	0.5924	0.5736	0.5623	0.4879
0.4	0.5439	0.6070	0.5515	0.5470	0.5015	0.4335
0.5	0.5387	0.6038	0.5094	0.5174	0.4334	0.3755
0.6	0.5420	0.5956	0.4688	0.4819	0.3612	0.3118
0.7	0.5521	0.5786	0.4293	0.4378	0.2859	0.2412
0.8	0.5634	0.5501	0.3867	0.3846	0.2053	0.1654
0.9	0.5655	0.5115	0.3344	0.3265	0.1165	0.0903

the numerical values of skin friction coefficient get declining trend.

6. Concluding remarks

The thermal properties of graphene oxide (GO) and molybdenum disulphide (MoS_2) nanoparticles have been discussed with help of fractional derivative approach. The engine oil is assumed as a base fluid for which the thermal performances are improved. The Atangana-Baleanu (AB) and Caputo-Fabrizio (CF) derivatives are followed to presents the numerical simulations. The accuracy of both schemes is verified. The main findings are:

- ➢ A decreasing change in the heat transfer rate is observed for the fractional parameters.
- ➢ The velocity profile improves with Grashof number while reverse velocity change has been noticed for fractional parameters.
- ➢ The temperature and velocity field of fractional model about overlaps to ordinary derivative model for $\alpha, \beta \rightarrow 1$.
- ➢ The nanoparticles temperature reduces with volume fraction coefficient.
- ➢ The profile of velocity simulated for AB-fractional model is relatively progressive as compared to CF-fractional model.
- ➢ The velocity profile of molybdenum disulphide based nanoparticles is a relatively greater than graphene oxide nanoparticles.

Declaration of competing interest

The authors declare that they have no known competing financial interests or personal relationships that could have appeared to influence the work reported in this paper.

Acknowledgment

The authors extend their appreciation to the Deanship of Scientific Research at King Khalid University, Abha, Saudi Arabia for funding this work through research groups program under grant number R.G.P-2/76/42.

References

[1] S.U.S. Choi, Enhancing thermal conductivity of fluids with nanoparticles, ASME-Publications-Fed 231 (1995) 99–106.
[2] Abuzar Abid Siddiqui, Mustafa Turkyilmazoglu, A new theoretical approach of wall transpiration in the cavity flow of the ferrofluids, Micromachines 10 (6) (2019) 373.
[3] Nadeem Abbas, S. Nadeem, Anber Saleem, M.Y. Malik, AlibekIssakhov, Fahd M. Alharbi, Models base study of inclined MHD of hybrid nanofluid flow over nonlinear stretching cylinder, Chin. J. Phys. 69 (February 2021) 109–117.
[4] S. Nadeem, Muhammad Israr-ur-Rehman, S. Saleem, Ebenezer Bonyah, Dual solutions in MHD stagnation point flow of nanofluid induced by porous stretching/shrinking sheet with anisotropic slip, AIP Adv. 10 (2020), 065207.
[5] Sami Ullah Khan, H. Waqas, M.M. Bhatti, M. Imran, Bioconvection in the rheology of magnetized Couple stress nanofluid featuring activation energy and Wu's slip, J. Non-Equilibrium Thermodyn. 45 (1) (2020) 81–95.
[6] M. Waqas, M. Mudassar Gulzar, A.S. Dogonchi, M. Asif Javed&W, A. Khan, Darcy–Forchheimer stratified flow of viscoelastic nanofluid subjected to convective conditions, Appl. Nanosci. 9 (2019) 2031–2037.
[7] R. Naveen Kumar, R.J. Punith Gowda, Mohammad Mahtab Alam, Irfan Ahmad, Y.M. Mahrous, M.R. Gorji, B.C. Prasannakumara, Inspection of convective heat transfer and KKL correlation for simulation of nanofluid flow over a curved stretching sheet, Int. Commun. Heat Mass Tran. 126 (July 2021) 105445.
[8] Sami Ullah Khan, Iskander Tlili, Waqas Hassan, Muhammad Imran, Effects of nonlinear thermal radiation and activation energy on modified second-grade nanofluid with Cattaneo–Christov expressions, J. Therm. Anal. Calorim. 143 (2021) 1175–1186.
[9] S.Mandal, G.C.Shit,Entropy analysis on unsteady MHD biviscosity nanofluid flow with convective heat transfer in a permeable radiative stretchable rotating , Chin. J. Phys., https://doi.org/10.1016/j.cjph.2021.07.036disk.
[10] Nilankush Acharya, Spectral quasi linearization simulation on the hydrothermal behavior of hybrid nanofluid spraying on an inclined spinning disk, Partial Differential Equations in Applied Mathematics 4 (December 2021) 100094.
[11] Yan Zhang, Nazia Shahmir, Muhammad Ramzan, Hammad Alotaibi, Hassan M. Aljohani, Upshot of melting heat transfer in a Von Karman rotating flow of gold-silver/engine oil hybrid nanofluid with Cattaneo-Christov heat flux, Case Studies in Thermal Engineering 26 (August 2021) 101149.
[12] Iftikhar Ahmad, Samaira Aziz, Nasir Ali, Sami Ullah Khan, Radiative unsteady hydromagnetic 3D flow model for Jeffrey nanofluid configured by an accelerated surface with chemical reaction, Heat Tran. Asian Res. 50 (1) (2021) 942–966.
[13] Hanumesh Vaidya, K.V. PrasadI. Tlili, O.D. Makinde, C. Rajashekhar, Sami Ullah Khan, Rakesh Kumar, D.L. Mahendr, Mixed convective nanofluid flow over a non linearly stretched Riga plate, Case Studies in Thermal Engineering 24 (April 2021) 100828.
[14] S.H. Pourhoseini, Maryam Ghodrat, Experimental investigation of the effect of Al_2O_3 nanoparticles as additives to B20 blended biodiesel fuel: flame characteristics, thermal performance and pollutant emissions, Case Studies in Thermal Engineering 27 (October 2021) 101292.
[15] Mohsan Hassan, Essam R. El-Zahar, Sami Ullah Khan, Mohammad Rahimi-Gorji, Ashfaq Ahmad, Boundary layer flow pattern of heat and mass for homogenous shear thinning hybrid-nanofluid: an experimental data base modeling, Numer. Methods Part. Differ. Equ. 37 (2) (March 2021) 1234–1249.
[16] R.J. Punith Gowda, A. Rauf, R. Naveen Kumar, B.C. Prasannakumara, S.A. Shehzad, Slip flow of Casson–Maxwell nanofluid confined through stretchable disks, Indian J. Phys. 2021 (2021), https://doi.org/10.1007/s12648-021-02153-7.
[17] Wasim Jamshed, R.J. Kottakkaran Sooppy Nisar, Punith Gowda, R. Naveen Kumar, B.C. Prasannakumara, Radiative heat transfer of second grade nanofluid flow past a porous flat surface: a single-phase mathematical model, Phys. Scripta 96 (6) (2021), 064006.
[18] R.J. Punith Gowda, R. Naveen Kumar, B.C. Prasannakumara, B. Nagaraja, B.J. Gireesha, Exploring magnetic dipole contribution on ferromagnetic nanofluid flow over a stretching sheet: an application of Stefan blowing, J. Mol. Liq. 335 (1 August 2021) 116215.
[19] R.S. Varun Kumar, R.J. Punith Gowda, R. Naveen Kumar, M. Radhika, B. C, PrasannakumaraTwo-phase flow of dusty fluid with suspended hybrid nanoparticles over a stretching cylinder with modified Fourier heat flux, SN Applied Sciences 3 (2021), 384.
[20] R.J. Punith Gowda, Fahad S. Al-Mubaddel, R. Naveen Kumar, B.C. Prasannakumara, Alibek Issakhov, Mohammad Rahimi-Gorji, Yusuf A. Al-Turki, Computational modelling of nanofluid flow over a curved stretching sheet using Koo–Kleinstreuer and Li (KKL) correlation and modified Fourier heat flux model, Chaos, Solitons & Fractals 145 (April 2021) 110774.
[21] L. Karthik, G. Kumar, T. Keswani, A. Bhattacharyya, S.S. Chandar, K.B. Rao, Protease inhibitors from marine actinobacteria as a potential source for antimalarial compound, PloS One 9 (3) (2014), e90972.

[22] N.A. Shah, I. Khan, Heat transfer analysis in a second grade fluid over and oscillating vertical plate using fractional Caputo–Fabrizio derivatives, The European Physical Journal C 76 (7) (2016) 1–11.
[23] S. Mondal, N.A. Haroun, P. Sibanda, The effects of thermal radiation on an unsteady MHD axisymmetric stagnation-point flow over a shrinking sheet in presence of temperature dependent thermal conductivity with Navier slip, PloS One 10 (9) (2015), e0138355.
[24] S. Aman, I. Khan, Z. Ismail, M.Z. Salleh, Applications of fractional derivatives to nanofluids: exact and numerical solutions, Math. Model Nat. Phenom. 13 (1) (2018) 2.
[25] M. Arif, P. Kumam, D. Khan, W. Watthayu, Thermal performance of GO-MoS2/engine oil as Maxwell hybrid nanofluid flow with heat transfer in oscillating vertical cylinder, Case Studies in Thermal Engineering (2021) 101290.
[26] Ying Qing Song Ali Raza, Kamel Al-Khaled, Saadia Farid, M. Ijaz Khan, Sami Ullah Khan, Qiu-HongShi, M.Y. Malik, M. Imran Khan, Significances of exponential heating and Darcy's law for second grade fluid flow over oscillating plate by using Atangana-Baleanu fractional derivatives, Case Studies in Thermal Engineering 27 (October 2021) 101266.
[27] Bing Guo, Raza Ali, Kamel Al-Khaled, Sami Ullah Khan, Saadia Farid, Ye Wang, M. Ijaz Khan, M.Y. Malik, S. Saleem, Fractional-order simulations for heat and mass transfer analysis confined by elliptic inclined plate with slip effects: a comparative fractional analysis, Case Studies in Thermal Engineering 28 (December 2021) 101359.
[28] M. Caputo, M. Fabrizio, A new definition of fractional derivative without singular kernel, Progr. Fract. Differ. Appl 1 (2) (2015) 1–13.
[29] A. Atangana, On the new fractional derivative and application to nonlinear Fisher's reaction–diffusion equation, Appl. Math. Comput. 273 (2016) 948–956.
[30] M. Abdullah, A.R. Butt, N. Raza, E.U. Haque, Semi-analytical technique for the solution of fractional Maxwell fluid, Can. J. Phys. 95 (5) (2017) 472–478.
[31] M.A. Khan, Z. Hammouch, D. Baleanu, Modeling the dynamics of hepatitis E via the caputo–fabrizio derivative, Math. Model Nat. Phenom. 14 (3) (2019) 311.
[32] V. Rajesh, Chemical reaction and radiation effects on the transient MHD free convection flow of dissipative fluid past an infinite vertical porous plate with ramped wall temperature, Chemical Industry and Chemical Engineering Quarterly/CICEQ 17 (2) (2011) 189–198.
[33] Raza Ali, Sami Ullah Khan, Saadia Farid, M. Ijaz Khan, Sun Tian-Chuan, Aamar Abbasi, M. Imran Khan, M.Y. Malik, Thermal activity of conventional Casson nanoparticles with ramped temperature due to an infinite vertical plate via fractional derivative approach, Case Studies in Thermal Engineering 27 (October 2021) 101191.
[34] Muhammad Mubashir Bhatti, S.U. Khan, O.A. Beg, A. Kadir, Differential transform solution for hall and Ion slip effects on radiative-convective Casson flow from a stretching sheet with convective heating, Heat Tran. Asian Res. 49 (2) (2020) 872–888.
[35] Nargis Khan, Iram Riaz, Muhammad Sadiq Hashmi, Saed A. Musmar, Sami Ullah Khan, Zahra Abdelmalek, Iskander Tlili, Aspects of chemical entropy generation in flow of Casson nanofluid between radiative stretching disks, Entropy 22 (5) (2020) 495.
[36] T. Hayat, S.A. Khan, M.I. Khan, A. Alsaedi, Optimizing the theoretical analysis of entropy generation in flow of second grade nanofluid, Phys. Scripta 94 (2019), 085001.
[37] M.I. Khan, F. Alzahrani, A. Hobiny, Z. Ali, Fully developed second order velocity slip Darcy-Forchheimer flow by a variable thicked surface of disk with entropy generation, Int. Commun. Heat Mass Tran. 117 (2020) 104778.
[38] T. Hayat, N. Aslam, M.I. Khan, M.I. Khan, A. Alsaedi, Physical significance of heat generation/absorption and Soret effects on peristalsis flow of pseudoplastic fluid in an inclined channel, J. Mol. Liq. 275 (2019) 599–615.
[39] M.I. Khan, F. Alzahrani, A. Hobiny, Z. Ali, Modeling of Cattaneo-Christov double diffusions (CCDD) in Williamson nanomaterial slip flow subject to porous medium, Journal of Materials Research and Technology 9 (2020) 6172–6177.
[40] M.I. Khan, F. ALzahrnai, Binary chemical reaction with activation energy in dissipative flow of non-Newtonian nanomaterial, J. Theor. Comput. Chem. 19 (2020) 2040006.